

[Click here to view linked References](#)

**PETROLOGICAL FEATURES OF THE FIRST CENOZOIC ALKALINE
MAGMATIC EVENT RECORDED IN NORTHWESTERN URUGUAY,
SOUTHERN EXTREME OF THE PARANÁ BASIN**

Muzio, R. ^(1*); Olivera, L. ⁽¹⁾; Fort, S. ⁽¹⁾; Peel, E. ⁽¹⁾

⁽¹⁾ Instituto de Ciencias Geológicas, Facultad de Ciencias.

Iguá 4225, CP 11400, Montevideo, Uruguay.

^(*) corresponding author: rossana@fcien.edu.uy

ABSTRACT

The Cenozoic mafic alkaline rocks found in northwestern Uruguay, in the southernmost portion of the Paraná Basin, comprise three subvolcanic plugs composed of Ne-tephrites. They cut through basalts that make up the Paraná Magmatic Province as well as part of the sandstones of the Late Jurassic–Early Cretaceous age. These mafic rocks are characterized by an aphanitic hypocrySTALLINE texture that is occasionally porphyritic with pyroxene and olivine macrocrysts/xenocrysts. We present the first lithogeochemical results that also include the Sr–Nd–Pb isotopes to determine the petrogenetic processes. These mafic rocks are enriched in light rare earth elements ($La/Lu_N = 23.12–28.81$) with respect to chondrite, in large-ion lithophile elements (Ba, U, and La), and in high-field-strength elements, such as Ta, Nb, and Zr, with respect to primitive mantle, and have a Mg# of 0.53–0.56. The trace element geochemistry and isotopic data (low radiogenic $^{206}Pb/^{204}Pb$ and low $^{87}Sr/^{86}Sr_i$ between 18.315 and 18.733, 0.70397 and 0.70443, respectively) indicate that the primary magma could be the product of the melting of an enriched mantle source with the possible involvement of metasomatic processes, lacking significant contamination by the continental crust. The K–Ar (whole rock) geochronology conducted on two samples yielded ages of 63.7 ± 2.5 and 51.5 ± 1.7 Ma for this magmatic event.

Keywords: alkaline rocks, geochemistry, isotopes, Cenozoic, Uruguay

1. INTRODUCTION

The widespread continental magmatism associated with the large igneous provinces is characterized as one of the largest and most extensive volcanic

expressions, with sub-volcanic intrusions accumulated over a short time (Renne et al., 1992; Coffin and Eldholm, 1994; Bryan and Ernst, 2008). In South America, the well-preserved Paraná Magmatic Province (PMP; Peate, 1997), with lava volumes of approximately $1,0 \times 10^6 \text{ km}^3$, infills and covers the Paraná Basin (PB) with an approximate area of $1,2 \times 10^6 \text{ km}^2$ over southern Brazil, eastern Paraguay, northern Argentina, and northwestern Uruguay (Piccirillo et al., 1988; Figure 1).

Regarding the petrology of the PMP, the predominance of tholeiitic basalts and related mafic intrusions can be highlighted. The age of the main tholeiitic magmatic activity of the PMP is constrained approximately 135–131 Ma (Renne et al., 1992 and Féraud et al., 1999, and from recalculated $^{40}\text{Ar}/^{39}\text{Ar}$ ages from Janasi et al., 2011). However, there are many records of the alkaline magmatic activity with a wide lithological and chemical variety (Ulbrich and Gomes, 1981; Milner et al., 1995; Huang et al., 1995; and later authors herein). In addition, alkaline magmatism can be found for different geochronological intervals, some of which are different ages than the main volcanic tholeiitic event of the PMP (Ulbrich and Gomes 1981; Comin-Chiramonti et al., 1991; Renne et al., 1993; Gomes et al., 1996; Gomes et al., 2003; Comin-Chiaramonti and Gomes, 2005a, b; Cernuschi et al., 2015; among others).

According to the geographic distribution and age, the record of alkaline pulses spanned from the Permo-Triassic until the Eocene, making up substantial number of alkaline provinces throughout Brazil, Paraguay, Argentina, Uruguay and Bolivia, mostly of Early-Late Cretaceous age (Litherland et al., 1986; Fletcher and Bleddoc-Stephens, 1987; Muzio, 2000; Comin-Chiaramonti and Gomes, 2005b; Cernuschi et al., 2015; Lagorio et al., 2016). In Paraguay, the alkaline

magmatic activity predates the tholeiitic volcanism of the PMP since the Permo-Triassic and spans until the Eocene (Gomes et al., 1996; Velázquez et al., 2006; Gomes et al., 2013). In addition, other alkaline complexes corresponding to Cenozoic magmatic events have been found in Brazil (Riccomini et al., 2005).

Both the lithological and chemical characteristics of these subvolcanic alkaline intrusions are significantly diverse. SiO₂-saturated to SiO₂-undersaturated rock series are common in most alkaline provinces, as well as the presence of potassic or sodic chemical affinity, including alkaline rocks such as lamproites, carbonatites and kimberlites (Biondi, 2005; Gomes and Comin-Chiaramonti, 2017).

One of the models suggested for the genesis of alkaline magmatism is the melting of metasomatized lithospheric mantle (Menzies and Murthy, 1980; Roden and Murthy, 1985; Bailey, 1987; among other authors). According to Beccaluva et al. (2008), the REE patterns, volatile concentrations, isotopes, and modelling of alkaline rocks and their xenoliths suggest that metasomatism plays a considerable role.

1.1. Nearby alkaline provinces in the region

At a regional scale, the alkaline provinces closest to Uruguay associated with the PB and with the Late Cretaceous – Eocene age are the Asunción (Paraguay), and Piratini Provinces (Rio Grande do Sul, Brazil; Figure 1).

The emplacement of the Asunción Province has been attributed to the Cenozoic evolution of the Asunción Rift (De Graff, 1985; Riccomini et al., 2001), which developed during the Paleogene between 68 and 52 Ma (Gomes et al., 2003). According to Riccomini et al. (2001), the ascent of the magmas would have

occurred through deep faults, whose activity caused a loss of energy in the asthenosphere, leading to melting of the asthenospheric mantle in a short period. The Asunción Province comprises plugs, necks, lavas and dikes of alkaline affinity, classified as ankaratrites, nephelinites, and subordinate peralkaline phonolites (Comin-Chiaramonti et al., 2013). Based on their isotopic signatures ($^{87}\text{Sr}/^{86}\text{Sr}=0.70362-0.70392$ and $^{143}\text{Nd}/^{144}\text{Nd}=0.51225-0.51242$), the sublithospheric mantle has been suggested as the origin (Comin-Chiaramonti et al., 1991; 1995: 1997). Analyses of the xenoliths hosted in these alkaline rocks indicate depths greater than 60 km for the genesis of these magmas (Comin-Chiaramonti et al., 1991). However, these rocks extend within the depleted quadrant ($\text{Sr}_i=0.70351$, $\text{Nd}_i=0.51273$), toward the HIMU and DMM compositional fields (Antonini et al., 2005). According to isotopic data, it has been inferred that from the Late Cretaceous until the Tertiary, depleted mantle domain(s) played a major role in the genesis of alkaline magmatism in eastern Paraguay (Comin-Chiaramonti et al., 1999). In addition, the Tertiary sodic rocks of Paraguay present the youngest values of T_{DM} in the region (approximately 500 Ma), suggesting a metasomatic event along the Late Proterozoic as a trigger mechanism for their genesis, according to Antonini et al. (2005).

The Late Cretaceous alkaline rocks corresponding to the Piratini Province (*sensu* Riccomini et al., 2005) comprise a considerable number of subvolcanic intrusions distributed in the Sul-Riograndense Shield, near the Piratini locality. Originally, they were known as the Rio Grande do Sul Alkaline Province (Ribeiro, 1971), and later as the Passo da Capela Alkaline Suite (e.g., Barbieri et al., 1987; da Silva, 2018) or Piratini Suite (Philipp et al., 2005; Gomes and Comin-Chiaramonti, 2017).

According to Almeida (1983), the ascent and emplacement of these alkaline rocks are associated with a Mesozoic – Cenozoic taphrogenic event, including old fault reactivation and new fault/fracture generation, in the Sul-Riograndense Shield, and are responsible for the opening of the South Atlantic Ocean. Moreover, subvolcanic intrusions and plugs are emplaced mostly along the NW structures (Burger et al., 1988).

The compositional diversity of this alkaline province ranges from tephrite-phonolites to phonolites and peralkaline phonolites (Barbieri et al., 1987), associated with a NE-SW olivine-diabase dike, with K-Ar ages between 99.3 and 76.0 Ma. This represents a late alkaline event in southernmost Brazil. Potassic and ultrapotassic dikes and pipes (lamproites and kimberlites) have also been found (Philipp et al., 2005).

The mean Sr-Nd isotope composition ($^{87}\text{Sr}/^{86}\text{Sr}_{(i)}=0.70533$; $^{143}\text{Nd}/^{144}\text{Nd}_{(i)}=0.51225-0.51230$) is in the same range as other Brazilian alkaline provinces and also of the spatially associated Early Cretaceous tholeiitic basalts of the southern PB (Piccirillo and Melfi, 1988). Crustal contamination has been discarded for these magmas by Vieira Jr. (1985), and their components are similar to those of the EMI mantle (Philipp et al., 2005).

1.2. Background in Uruguay

The exposed volcanic areas of the PB in Uruguay are represented by tholeiitic basalt lava flows and related mafic intrusions, which are restricted to the Lower Cretaceous (Creer et al., 1965; Turner et al., 1999; Muzio et al., 2017). Until recently, the occurrence of Uruguayan Na-alkaline rocks related to the Gondwana break-up has been restricted to the southeastern Laguna Merin Basin (Figure 1), associated with the Santa Lucia-Aiguá-Merin lineament (Rossello et

al., 2000) and the South Atlantic Ocean opening. They comprise SiO₂-saturated rocks (quartz syenites, syenites, granites, and rhyolites), included in the Valle Chico and Lascano alkaline complexes, all of which have an Early Cretaceous age (Muzio, 2000; Lustrino et al., 2005; Cernuschi et al., 2015). Based on their chemical and isotopic compositions, an enriched mantle source with EMI components has been assigned (Lustrino et al., 2005; Cernuschi et al., 2015). Neither SiO₂-undersaturated nor younger alkaline rocks have been reported to date in Uruguay.

Recent studies have demonstrated the occurrence of mafic subvolcanic rocks that crosscut the basaltic pile filling the Uruguayan portion of the PB, classified as Ne-tephrites by Olivera (2019) and Muzio et al. (2019).

This study aims to present the main petrological features of the youngest and first reported SiO₂-undersaturated alkaline magmatism found in Uruguay, in the extreme southernmost region of the PB.

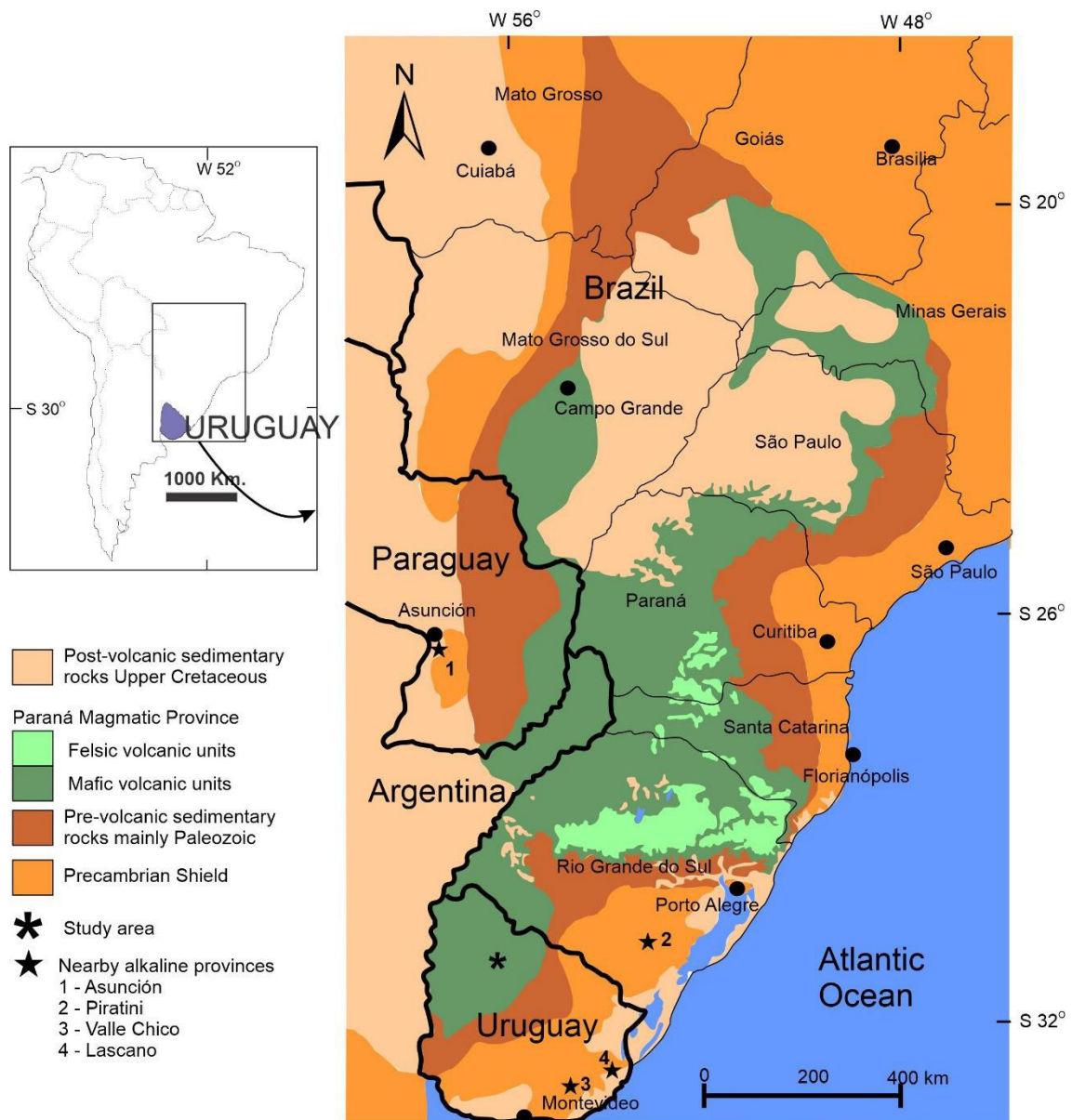


Figure 1 – Simplified geological map of the Paraná Basin, with the regional location of the Paraná Magmatic Province and the main alkaline provinces close to Uruguay (modified after Piccirillo et al., 1988; Renner et al., 2011).

2. GEOLOGIC FRAMEWORK

The northwestern region of Uruguay is geologically underlain by the southern portion of the PB (Cordani et al., 1984), which is locally known as the Norte Basin (NB, Ucha and de Santa Ana, 1994; Figure 2a). The sedimentary pile comprises

Devonian to Late Cretaceous sedimentary sequences intercalated with Early Cretaceous rocks related to the PMP. More than 40,000 km² of lava flows are well exposed in this basin, as well as part of the related mafic intrusions (Muzio et al., 2017). The volcanic sedimentary rock package corresponds to the Gondwana III super sequence (Milani et al., 2007) and is represented by the Tacuarembó Formation (Bossi, 1966) and PMP-related volcanic and intrusive units. The Tacuarembó Formation comprises fluvial and aeolian sandstones of the Late Jurassic–Early Cretaceous age, and is correlated with the Botucatu Formation (Almeida, 1954; Salamuni and Bigarella, 1967) in Brazil. The magmatism of basaltic composition and tholeiitic nature is represented by the lava flows of the Arapey Formation (Bossi, 1966), and the related mafic intrusive bodies (dikes and sills) included in the Cuaró Formation (Preciozzi et al., 1985). These volcanic and mafic intrusive units correlate with those of the Serra Geral Formation of the PMP (Peate, 1997).

The studies conducted by Soto (2014) near the Pepe Núñez region (East Salto Department, Uruguay, Figure 2) suggested the presence of “infrequent mafic lithotypes,” which were interpreted as possible volcanic necks or conduits. Subsequent studies, comprising detailed petrographic sampling and geochemistry (Olivera, 2019; Muzio et al., 2019), along with the data presented in this study, help to confirm the occurrence of a different magmatic event from that recognized for the PMP basalts. The study area in the present work is located 490 km northwest from Montevideo (Figure 2b).

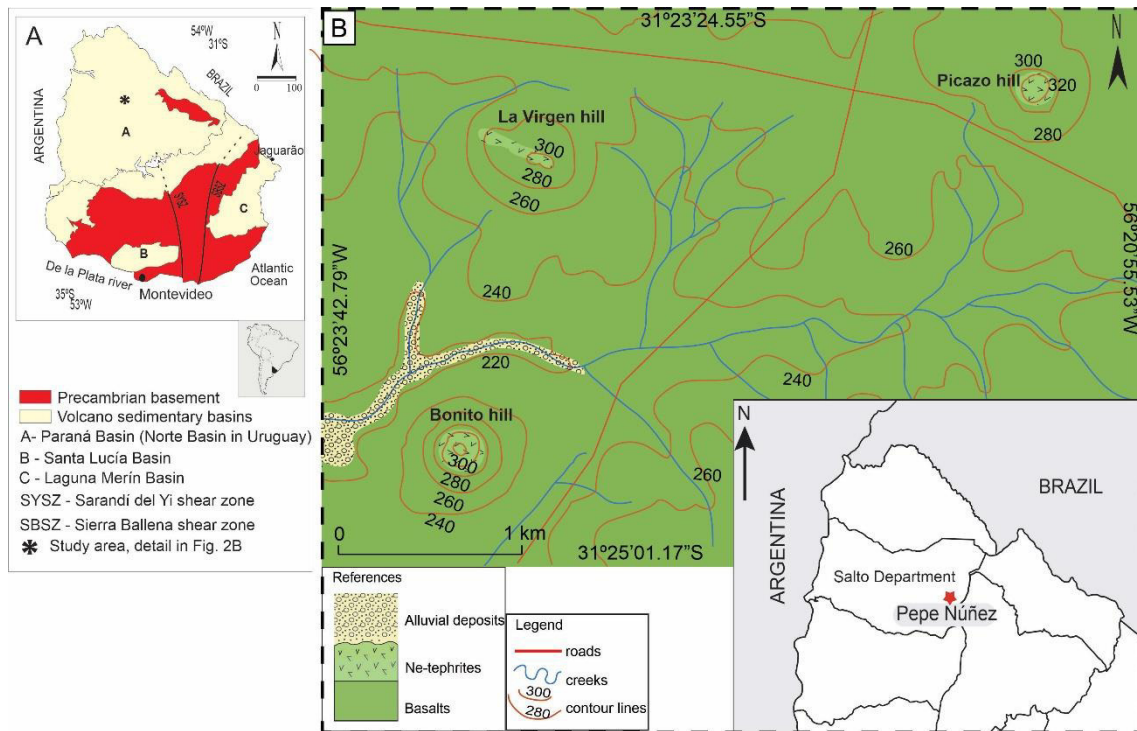


Figure 2 – (a) Location map with the main structural framework and (b) simplified geological map of the study region, northwestern Uruguay (Olivera, 2019).

The rocks of interest crop out of the basalts of the Arapey Formation, and partially out of the sandstones of the Tacuarembó Formation. Owing to soil coverage, no thermal features were observed in the surrounding basalts or sandstones. They make up three rounded to elliptical hills locally named Bonito, La Virgen, and Picazo (Figure 2b), with a mean height of approximately 300 m above sea level and maximum dimensions for their major axis or diameters of approximately 500 m, exhibiting a marked columnar disjunction. All the rocks are dark black and exhibit an aphanitic hypocrySTALLINE texture that is occasionally porphyritic with pyroxene (augite) and Mg-rich olivine macrocrysts/xenocrysts (less than 10% in content, with a mean size of 3 mm). The groundmass was composed of olivine, augite, nepheline, and opaque minerals (predominantly ulvospinel and pyrite). Qualitative compositional estimations have also been assessed using scanning

electron microscopy–energy-dispersive spectroscopy, particularly for nepheline and opaque minerals (Olivera and Muzio, 2019). No other internal textural variations were observed in any of the hills, which allowed the separation of the petrographic facies.

3. METHODOLOGY

Two samples (Table 1) were dated using K–Ar (whole rock) at ACTLABS Laboratories (Ontario, Canada). For the analysis, aliquots of the samples were weighed into Al containers, loaded into the sample system of the extraction unit, and degassed at approximately 100°C for 2 days to remove the surface gases. Ar was extracted from the samples in a double-vacuum furnace at 1700°C. The radiogenic Ar content was determined twice on an MI-1201 IG mass spectrometer using the isotope dilution method with ³⁸Ar, which was spiked into the sample system prior to each extraction. The extracted gases were cleaned in a two-step purification system, and then, pure Ar was introduced into a custom-built magnetic sector mass spectrometer (Reinolds type). The K content was determined via flame photometry using an FPA-01 spectrometer.

The tests were performed twice for each sample to ensure consistency of the results. The final values provided by ACTLABS in Table 1 represent the average values for each sample. Two globally accepted standards (P-207 muscovite and 1/65 “Asia” rhyolite matrix) were used for ³⁸Ar spike calibration. For the age calculations, the international values of the constants were used as follows: $\lambda_K = 0.581 \times 10^{-10} \text{y}^{-1}$, $\lambda_{\beta^-} = 4.962 \times 10^{-10} \text{y}^{-1}$, and $^{40}\text{K} = 0.01167 \text{ (at.%)}$.

Sample	Location	latitude	longitude	%K ± σ	⁴⁰ Ar rad (ng/g)	% ⁴⁰ Ar air	Age (My)	error 2σ
CV04	La Virgen hill	31°23'47.05"S	56°23'6.44"W	1.24 ± 0.02	5.58 ± 0.08	47.6	63.7	2.5
CB10	Bonito hill	31°24'46.14"S	56°23'19.06"W	0.970 ± 0.015	3.51 ± 0.02	30	51.5	1.7

Table 1 – Results of K-Ar dating (whole rock).

Nine samples with no visible secondary alteration were selected for lithochemical analyses. All the samples were carefully cleaned, crushed, and pulverized at the Instituto de Ciencias Geológicas (Montevideo). Major and trace elements were analyzed by the ACME-Bureau Veritas Laboratories (Vancouver, Canada), following the LF-202 Litho-Research package methodology. Ba, Sr, Y, Sc, Zr, V, and Be were analyzed using inductively coupled plasma atomic emission spectrometry (ICP-AES). Trace elements (including REE) were determined via ICP mass spectrometry (ICP-MS). The analytical protocol at the ACME Laboratory included an analysis of the reference material STD-SO-19. All the lithochemical and isotope data were processed using the GCDkit 6.0 software (Janousek et al., 2006). The whole-rock analyses were recalculated to 100% on an anhydrous basis and are presented in Table 2.

Sample code	CV00	CV02	CV04B	CV06	CP03	CP07	CB00	CB06	CB09
latitude	31°23'50.81S	31°23'45.20S	31°23'47.05S	31°23'49.97S	31°23'40.32S	31°23'37.90S	31°24'46.02S	31°24'42.81S	31°24'44.39S
longitude	56°22'58.17W	56°23'9.96W	56°23'6.44W	56°23'0.01W	56°21'13.69W	56°21'15.72W	56°23'16.48W	56°23'15.59W	56°23'18.52W
SiO ₂	41.44	42.14	41.88	41.75	44.26	43.10	41.50	40.83	40.89
Al ₂ O ₃	12.78	12.89	12.80	12.89	12.64	12.82	13.05	12.70	12.91
Fe ₂ O ₃	13.93	13.50	13.54	13.91	13.00	13.23	14.01	14.03	13.80
MgO	8.06	7.96	8.42	8.12	8.11	8.49	8.43	8.81	8.82
CaO	12.49	12.43	12.23	12.19	12.12	11.85	12.63	13.01	12.89
Na ₂ O	5.11	4.87	4.64	4.63	3.45	4.16	3.93	4.26	4.52
K ₂ O	1.18	1.21	1.56	1.66	2.01	1.87	1.44	1.36	0.98
TiO ₂	2.50	2.48	2.45	2.42	2.20	2.27	2.57	2.49	2.50
P ₂ O ₅	1.78	1.73	1.71	1.71	1.49	1.49	1.63	1.74	1.80
MnO	0.22	0.20	0.21	0.21	0.20	0.20	0.20	0.21	0.21
Cr ₂ O ₃	0.02	0.02	0.02	0.02	0.02	0.02	0.02	0.02	0.01
Ba	786.00	858.00	789.00	797.00	771.00	760.00	821.00	730.00	831.00
Ni	64.60	64.30	63.50	66.10	80.10	80.20	67.10	62.90	58.60
Sc	18.00	18.00	18.00	18.00	18.00	18.00	19.00	18.00	18.00
Be	2.00	3.00	5.00	<1	2.00	2.00	6.00	<1	<1
Co	59.50	79.90	73.70	70.10	75.00	85.20	107.10	95.80	95.00
Cs	1.00	0.90	1.00	1.00	0.80	0.80	0.70	0.90	0.90
Ga	19.90	19.40	18.70	18.90	17.70	18.50	18.70	12.40	13.00
Hf	8.10	8.30	8.20	8.00	7.80	7.80	6.90	7.00	7.20
Nb	76.40	77.40	77.80	76.60	69.40	70.80	66.50	72.20	72.60
Rb	42.00	40.20	59.80	55.30	57.70	53.30	37.40	65.00	38.90
Sn	2.00	2.00	2.00	3.00	2.00	2.00	2.00	2.00	2.00
Sr	1480.30	1476.90	1480.00	1426.80	1366.40	1355.80	1579.00	1390.50	1416.70
Ta	5.20	5.40	5.40	5.30	4.90	5.10	6.20	5.90	5.80
Th	6.20	6.00	6.00	6.30	6.50	6.70	4.90	5.20	5.50
U	2.00	2.10	2.10	2.30	2.40	2.30	2.50	2.40	2.70
Pb	3.50	3.70	3.60	3.60	4.00	3.80	2.30	3.20	3.10
Zn	122.00	109.00	110.00	108.00	102.00	98.00	99.00	95.00	98.00
V	167.00	167.00	168.00	166.00	159.00	165.00	175.00	198.00	197.00
W	156.30	269.90	242.00	207.20	222.80	209.30	337.50	231.50	348.60
Zr	411.60	413.90	430.60	410.50	393.60	407.70	356.80	358.20	369.30
Y	32.60	32.10	33.40	32.30	29.70	31.30	33.50	34.90	37.30
La	84.80	83.90	85.60	83.20	75.70	77.50	78.30	77.90	80.20
Ce	164.40	164.60	169.10	169.50	149.10	155.80	154.30	156.90	161.60
Pr	18.65	18.49	18.66	18.45	16.58	17.26	17.78	18.58	19.36
Nd	72.50	71.10	72.10	73.30	65.00	68.10	71.30	73.40	79.30
Sm	12.99	12.83	13.48	13.32	12.13	11.86	13.20	13.77	13.86
Eu	3.89	3.91	4.09	3.99	3.60	3.71	3.98	4.14	4.26
Gd	11.23	11.11	11.28	11.26	10.27	10.33	11.34	12.23	12.60
Tb	1.48	1.47	1.50	1.48	1.33	1.38	1.49	1.56	1.63
Dy	7.49	7.40	7.67	7.36	6.68	6.80	7.80	7.55	8.34
Ho	1.22	1.28	1.23	1.26	1.20	1.18	1.30	1.32	1.39
Er	2.94	3.16	3.12	3.13	2.88	2.85	3.37	3.24	3.44
Tm	0.38	0.37	0.36	0.36	0.36	0.37	0.40	0.42	0.44
Yb	2.24	2.40	2.39	2.20	2.20	2.21	2.37	2.57	2.48
Lu	0.31	0.32	0.32	0.30	0.31	0.31	0.33	0.35	0.35
mg#	0.53	0.54	0.55	0.54	0.55	0.54	0.53	0.55	0.56
LOI	3.20	1.90	2.50	2.80	3.20	2.70	1.70	1.30	1.60
Sum	99.60	99.58	99.58	99.60	99.61	99.61	99.56	99.50	99.47

Table 2 – Geochemical data for the Ne-tephrites from northwestern Uruguay.

References: CV – La Virgen hill; CP – Picazo hill and, CB – Bonito hill.

The Nd–Sr–Pb isotopic analyses of six freshly selected samples were conducted at the Geochronological Research Center (CPGeo-USP) at the University of São Paulo, Brazil. All the interpreted isotopic data and locations of the samples are listed in Table 3. The Nd analysis was conducted using an ICP-MS Thermo-Neptune mass spectrometer.

Sample	latitude	longitude	$^{87}\text{Sr}/^{86}\text{Sr}_{(0)}$	error (2σ)	$^{87}\text{Sr}/^{86}\text{Sr}_{(i)}$	
CP - 03	31°23'40.32S	56°21'13.69W	0.70453	0.000021	0.70406	
CP - 07	31°23'37.90S	56°21'15.72W	0.70424	0.000015	0.70403	
CV - 04b	31°23'47.05S	56°23'6.44W	0.70416	0.000020	0.70443	
CV - 06	31°23'49.97S	56°23'0.01W	0.70412	0.000024	0.70414	
CB - 06	31°24'42.81S	56°23'15.59W	0.70409	0.000017	0.70398	
CB - 09	31°24'44.39S	56°23'18.52W	0.70403	0.000018	0.70397	

Sample	$^{143}\text{Nd}/^{144}\text{Nd}_{(0)}$	error (2σ)	$\epsilon\text{Nd}_{(0)}$	$\epsilon\text{Nd}_{(i)}$	$^{143}\text{Nd}/^{144}\text{Nd}_{(i)}$	T_{DM}
CP - 03	0.512635	0.000005	-0.05805986	0.600000	0.512594	0.740
CP - 07	0.512634	0.000006	-0.07444574	0.970000	0.512614	0.693
CV - 04b	0.512637	0.000006	-0.01904587	0.560000	0.512592	0.741
CV - 06	0.512655	0.000005	0.322326578	0.590000	0.512594	0.694
CB - 06	0.512665	0.000005	0.526759908	1.140000	0.512622	0.702
CB - 09	0.512660	0.000005	0.429029852	1.100000	0.512620	0.661

Sample	$^{206}\text{Pb}/^{204}\text{Pb}$	error (2σ)	$^{207}\text{Pb}/^{204}\text{Pb}$	error (2σ)	$^{208}\text{Pb}/^{204}\text{Pb}$	error (2σ)
CP - 03	18.315	0.005241	15.505	0.004665	38.500	0.011023
CP - 07	18.364	0.008052	15.506	0.007656	38.507	0.022197
CV - 04b	18.495	0.005996	15.519	0.006309	38.603	0.018973
CV - 06	18.448	0.007302	15.517	0.006413	38.555	0.016176
CB - 06	18.718	0.005287	15.527	0.004494	38.548	0.011653
CB - 09	18.733	0.007646	15.527	0.008122	38.550	0.022055

Table 3 – Sr - Nd – Pb isotopic compositions for the Ne-tephrites from northwestern Uruguay. Initial ratios for Sr, Nd and epsilon values were calculated to a mean age of 57.6 Ma. References: CV – La Virgen hill; CP – Picazo hill and, CB – Bonito hill.

The isotopic ratios of $^{143}\text{Nd}/^{144}\text{Nd}$ (measured as Nd+) were normalized to $^{146}\text{Nd}/^{144}\text{Nd} = 0.7219$ (De Paolo, 1981), and the $^{143}\text{Nd}/^{144}\text{Nd}$ average for the JNDi-

1 standard was 0.512102 ± 0.000003 (2σ). The $\epsilon\text{Nd}_{(0)}$ parameter corresponds to the actual value ($t = 0$) and was calculated according to the equation: $\epsilon\text{Nd}_{(0)} = \{[(^{143}\text{Nd}/^{144}\text{Nd})_{\text{a.m.u.}}/0.512638]-1\} \times 1 \times 10^4$, where $^{143}\text{Nd}/^{144}\text{Nd}_{\text{CHUR}} = 0.512638$ (Hamilton et al., 1983). The analytical blanks were approximately 202 pg.

The Sr isotope analyses were conducted using TIMS-Thermo Triton equipment. The $^{87}\text{Sr}/^{86}\text{Sr}$ isotopic ratios were normalized to $^{86}\text{Sr}/^{88}\text{Sr} = 0.1194$, with analytical blanks of 178 pg. The mean value used to determine the $^{87}\text{Sr}/^{86}\text{Sr}$ ratio was the NBS-987 pattern of 0.710248 ± 0.000016 (2σ), which corresponds to June 2017 to May 2018.

The Pb isotopic determinations were performed using a TIMS–Finnigan MAT 262 equipment. The isotopic ratios were corrected for 0.12%/a.m.u. mass fractionation ($^{207}\text{Pb}/^{204}\text{Pb}$ ratio) and 0.13%/a.m.u. mass fractionation ($^{206}\text{Pb}/^{204}\text{Pb}$ and $^{208}\text{Pb}/^{204}\text{Pb}$ ratios). The mean values used for the isotopic ratios of the NBS-981 standard were $^{206}\text{Pb}/^{204}\text{Pb} = 16.891 \pm 0.005$, $^{207}\text{Pb}/^{204}\text{Pb} = 15.429 \pm 0.007$, and $^{208}\text{Pb}/^{204}\text{Pb} = 36.503 \pm 0.022$. The blanks used during the Pb analysis were approximately 100 pg.

4. RESULTS

4.1. K–Ar geochronology

The analytical data from the K–Ar dating (whole rock) are presented in Table 1. Two samples were dated (CV-04 and CB-010 from Virgen Hill and Bonito Hill, respectively; see Figure 2). The ages obtained (63.7 ± 2.5 and 51.5 ± 1.7 Ma) are the first documented dates for magmatic activity during the Cenozoic (Paleocene–Early Eocene), both in the Norte Basin and for all of Uruguay.

4.2. Lithogeochemistry

Chemical data of the analyzed samples and corresponding location are given in Table 2.

The samples present the following chemical compositions: SiO₂ ranging from 40.83 to 44.26 wt %, TiO₂ from 2.20 to 2.57 wt%, Al₂O₃ from 12.64 to 13.05 wt%, Fe₂O₃ from 13.00 to 14.03 wt%, MgO from 7.96 to 8.82 wt. %, CaO from 11.85 to 13.01 wt%, Na₂O from 3.45 to 5.11 wt%, K₂O from 0.98 to 2.01 wt%, and P₂O₅ from 1.49 to 1.80 wt%. The Mg# varies from 0.53 to 0.56.

According to the classification diagram presented by Le Bas et al. (1986), all the samples lie in the basanite–tephrite field (Figure 3). Based on the normative olivine content (less than 10%; following Le Maître, 2002), and on previous studies developed by Olivera (2019), the samples classify as Ne-tephrites.

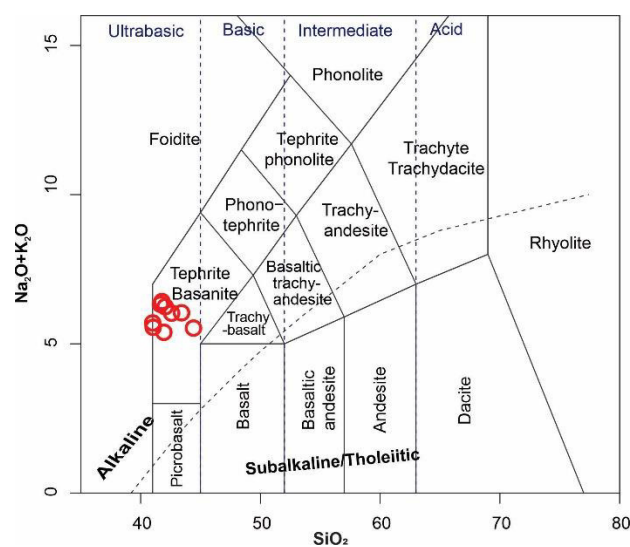


Figure 3 – Classification diagram for the Ne-tephrites, according to Le Bas et al. (1986).

Because this is the first documented report of Cenozoic SiO₂-subsaturated alkaline rocks in Uruguay, we compared the chemical data with nearby alkaline complexes of similar ages. Therefore, available data from the Piratini (Late Cretaceous), and Asunción (Eocene) provinces, were considered.

The sodic affinity of the Ne-tephrites is presented in the K_2O vs. Na_2O classification diagram (Figure 4), sharing not only the sodic nature but also the rank of ages with the sodic alkaline rocks of the Asunción Province. These alkaline rocks from Paraguay are spatially near those of the present study and exhibit similar chemical features and ages, which are restricted to a time window between 66 and 33 Ma (Chiaramonti et al., 1997; Comin-Chiaramonti et al., 2007b; Comin-Chiaramonti et al., 2013). Hereafter, we continue to use the chemical data to compare the Ne-tephrites with the Paraguayan sodic alkaline rocks.

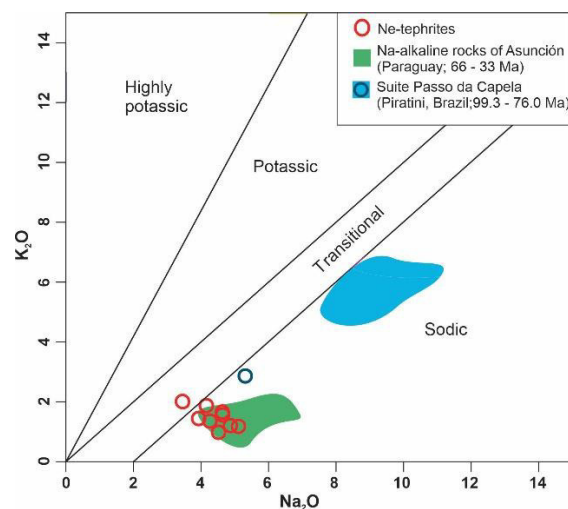


Figure 4 – Classification diagram for the Ne-tephrites, according to the distribution of K_2O vs. Na_2O (Middlemost, 1975). The shaded areas represent average values for the Na-alkaline rocks of Asunción (Eocene) and Piratini Provinces (Late Cretaceous); taken from Comin-Chiaramonti et al. (1991); Comin-Chiaramonti et al. (2013) and da Silva (2018).

The Ne-tephrites are enriched in large-ion lithophile elements and high field strength elements in the multielement diagram compared with the primitive mantle (Figure 5a; Sun and McDonough, 1989). Negative K and Ti anomalies were clearly observed, coupled with positive peaks of Ba, U, Ta, La, P, and Zr. Furthermore, in Figure 5b, a mild enrichment in light rare earth elements (LREE)

($La/Lu_N = 23.12\text{--}28.81$) is observed, with $\Sigma REE = 347.34\text{--}390.90$, normalized to chondrite values (Boynton, 1984). A range of values of incompatible elements with respect to the primitive mantle is expected for rocks with alkaline affinity.

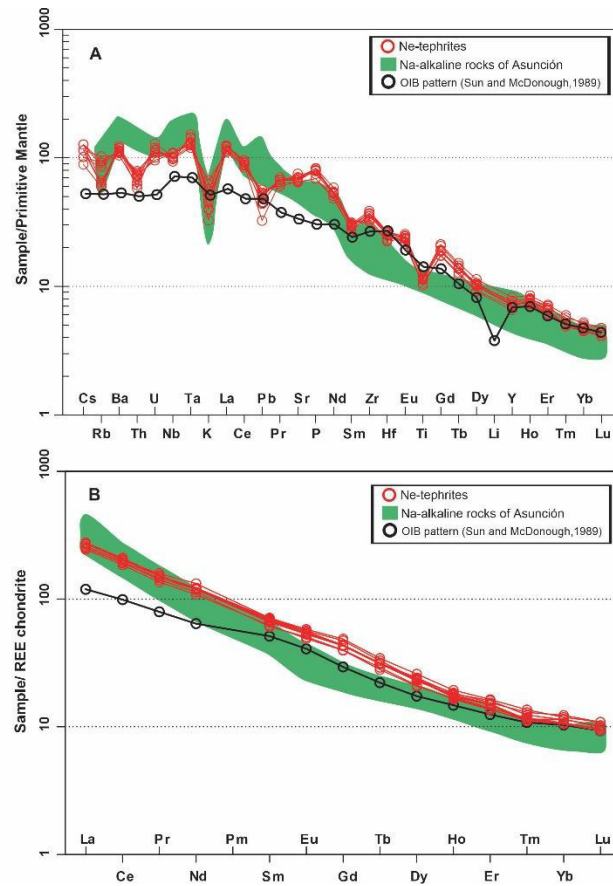


Figure 5 – Multielement diagram and REE patterns for the Ne-tephrites normalized according to (a) Primitive mantle (Sun and Mc Donough, 1989); (b) Chondrite (Boynton, 1984). The shaded areas in green represent average values for the Na-alkaline rocks of Asunción, taken from Comin-Chiaramonti et al. (1991); Comin-Chiaramonti et al. (2013).

Eu anomalies are not observed for the Ne-tephrites, which present values between 0.98 and 1.03 ($Eu/Eu^* = Eu_N/[Sm_N \times Gd_N]^{0.5}$). As shown in Figure 6, the Ne-tephrites lie within the mantle array at values corresponding to MORB-OIB sources, suggesting an enriched source for the genesis of this magma and

reinforcing the geochemical signature defined by the incompatible element pattern.

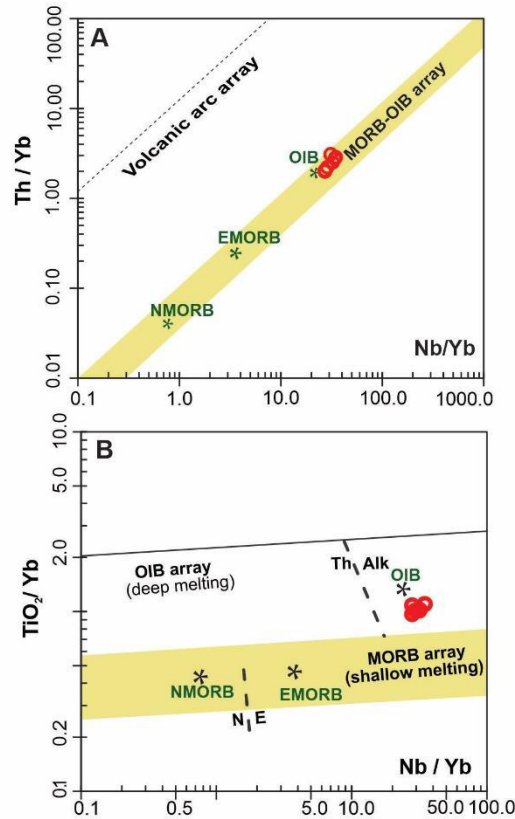


Figure 6 –(a) Th/Yb vs. Nb/Yb and (b) TiO₂ vs. Nb/Yb incompatible element ratio diagrams for the Ne-tephrites, after Pearce (2008).

4.3. Isotope geochemistry

The analytical results obtained for Sr, Nd, and Pb are presented in Table 3 and Figures 7–9. The initial ⁸⁷Sr/⁸⁶Sr and ¹⁴³Nd/¹⁴⁴Nd ratios were calculated to an age of 57.6 Ma (mean age value).

The initial values of the ⁸⁷Sr/⁸⁶Sr and ¹⁴³Nd/¹⁴⁴Nd ratios ranged from 0.70398 to 0.70443 and 0.512592 to 0.512622, respectively. The epsilon neodymium values range from +0.56 to +1.14, with T_{DM} ages between 661 and 741 Ma. According to the diagram presented in Figure 7, all the samples lie in the DM - PREMA array

(Stracke, 2012). The isotopic data closely resembles to the source of the coeval sodic alkaline rocks from Paraguay (area in green).

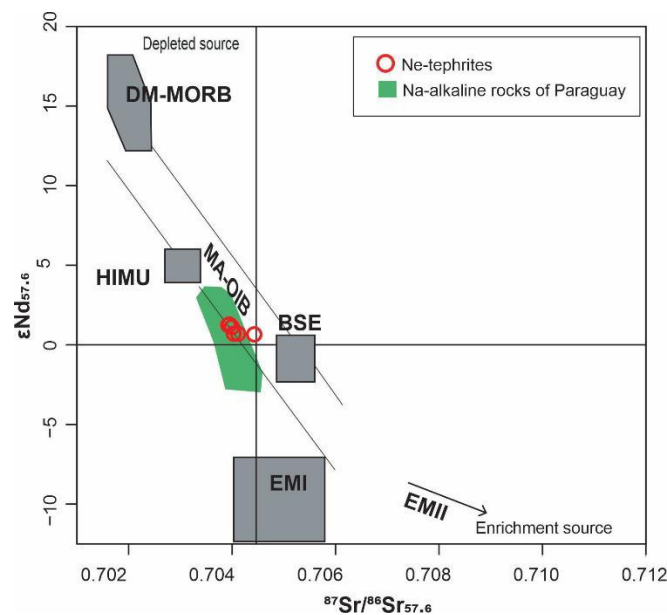


Figure 7 – Initial $^{87}\text{Sr}/^{86}\text{Sr}$ vs. $^{143}\text{Nd}/^{144}\text{Nd}$ diagram for the Ne-tephrites from Uruguay, modified after De Paolo and Wasserburg (1979) and Zindler and Hart (1986). The shaded area in green represents average values for contemporary sodic alkaline rocks from Paraguay (taken from Gomes et al., 2013). References: MORB: Mid Ocean Ridge Basalts, DM: Depleted Mantle, MA-OIB: Mantle Array- Ocean Island Basalts, BSE: Bulk Silicate Earth, HIMU: High μ mantle component ($\mu=^{238}\text{U}/^{204}\text{U}$), EM (I, II): Enriched Mantle.

The present-day Pb isotope compositions ranged from 18.315 to 18.733 for $^{206}\text{Pb}/^{204}\text{Pb}$, 15.505 to 15.527 for $^{207}\text{Pb}/^{204}\text{Pb}$, and 38.500 to 38.603 for $^{208}\text{Pb}/^{204}\text{Pb}$ (Figure 8).

In both the $^{206}\text{Pb}/^{204}\text{Pb}$ vs. $^{87}\text{Sr}/^{86}\text{Sr}$ and $^{206}\text{Pb}/^{204}\text{Pb}$ vs. $^{143}\text{Nd}/^{144}\text{Nd}$ diagrams (Figure 9), the studied rocks exhibit similar behaviors and lie close to the PREMA/BSE mantle reservoir field.

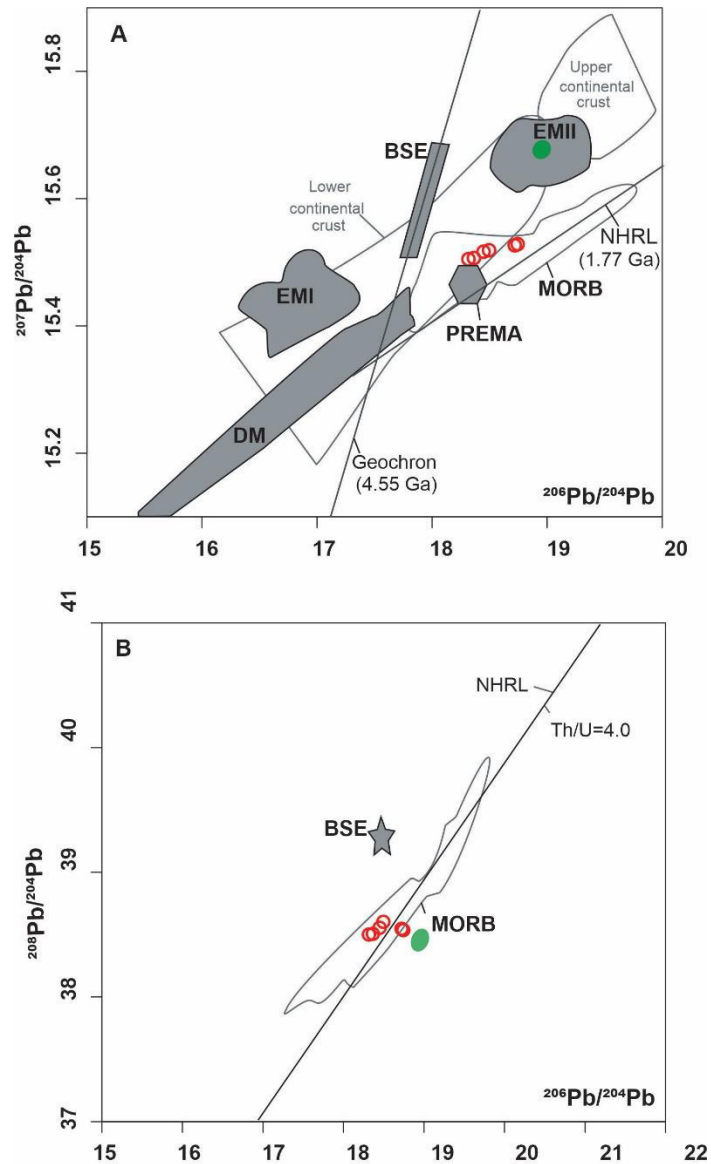


Figure 8 – (a) $^{207}\text{Pb}/^{204}\text{Pb}$ vs. $^{206}\text{Pb}/^{204}\text{Pb}$ and (b) $^{208}\text{Pb}/^{204}\text{Pb}$ vs. $^{206}\text{Pb}/^{204}\text{Pb}$ isotope compositions for the Ne-tephrites compared to mantle components (Zindler and Hart, 1986). NHRL – Northern Hemisphere Reference Line (Hart, 1984). The shaded area in green represents average values for contemporary sodic alkaline rocks from Paraguay (taken from Gomes et al., 2013). References: MORB: Mid Ocean Ridge Basalts, DM: Depleted Mantle, BSE: Bulk Silicate Earth, PREMA: Prevalent Mantle, EM (I, II): Enriched Mantle.

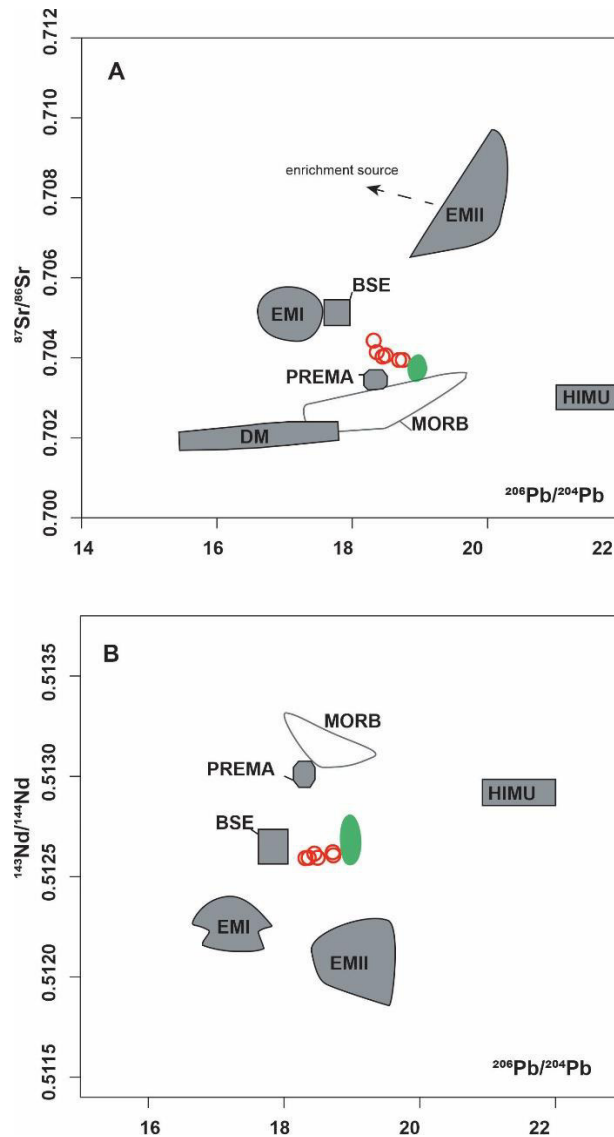


Figure 9 – (a) $^{87}\text{Sr}/^{86}\text{Sr}_{(i)}$ vs. $^{206}\text{Pb}/^{204}\text{Pb}$ and (b) $^{143}\text{Nd}/^{144}\text{Nd}_{(i)}$ vs. $^{206}\text{Pb}/^{204}\text{Pb}$ isotope compositions for the Ne-tephrites compared to the fields of mantle components (Zindler and Hart, 1986). The shaded area in green represents average values for contemporary sodic alkaline rocks from Paraguay (taken from Gomes et al., 2013). References: MORB: Mid Ocean Ridge Basalts, DM: Depleted Mantle, BSE: Bulk Silicate Earth, PREMA: Prevalent Mantle, EM (I, II): Enriched Mantle, HIMU: High μ mantle component ($\mu=^{238}\text{U}/^{204}\text{U}$).

5. DISCUSSION

The ultramafic Na-alkaline rocks found in northwestern Uruguay, described herein, are restricted in composition to Ne-tephrites, indicating no evidence of magmatic differentiation processes. One diagnostic feature of the multielement

diagram normalized to chondrite (Figure 5a) is the negative K anomaly. Late Cretaceous to Tertiary sodic alkaline rocks generally differ from other alkaline rocks because of the presence of a strong negative anomaly of K, and positive anomalies of Nb, P, and Y (Antonini et al. (2005). According to Comin-Chiaramonti et al. (1997), this anomaly can be explained by the residual phase of phlogopite in the mantle source.

Other chemical features, such as the enrichment the of Ba, U, and La, and HFS elements, such as Zr, Ta and Nb, are common in rocks derived from alkaline magmas.

Diagrams combining the isotopes and major and trace element data were used to discuss the possible processes that occurred during the ascent and crystallization of the Na-alkaline magma, as demonstrated in Figure 10. As shown in Figures 10a and 10b, all the samples exhibit Fractional Crystallization (FC) trends. In addition, a P_2O_5/K_2O vs. $\epsilon Sr_{(i)}$ diagram was used (Figure 10c). Depending on the P_2O_5/K_2O ratio, mantle-derived rocks typically exhibit high ratios, that are greater than 0.1 (Carlson and Hart, 1987; Hart et al., 1997). The FC trend and values above 0.5, together with the Rb/Ba ratios between 0.05 and 0.09, indicate that they have undergone no significant crustal contamination (Rudnick and Fountain, 1995).

All samples had a SiO_2 -subsaturated alkaline characteristic that can be related to an OIB-like mantle source. The isotopic signatures (such as low radiogenic $^{206}Pb/^{204}Pb$ and low values of $^{87}Sr/^{86}Sr_{(i)}$) point to an enriched mantle source, similar to the PREMA or BSE mantle components, following the DM-PREMA array field (Figure 7 and 9). Considering that the samples lack crustal contamination, the $Sr_{(i)}$ and $Nd_{(i)}$ compositions of the Ne-tephrites may be

preserved and considered as representative of the isotopic composition of the mantle source.

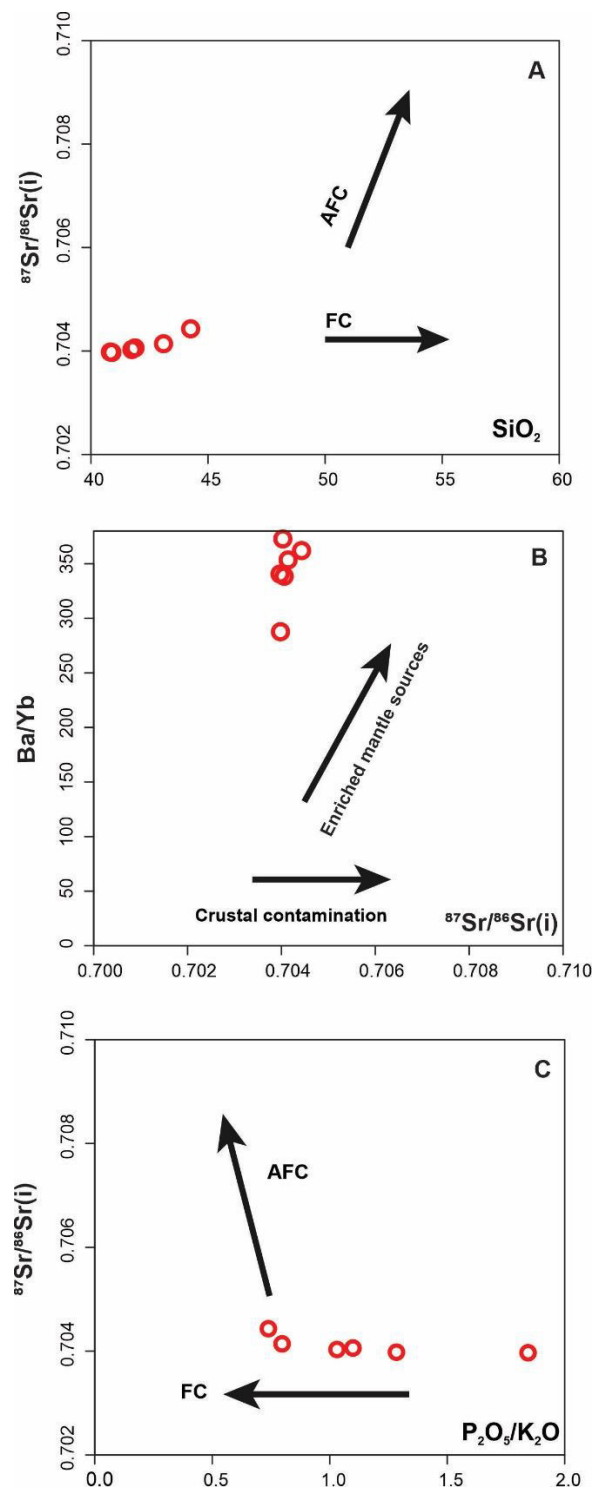


Figure 10 – Indicative diagrams to evaluate crustal contamination. (a) Ba/Yb vs. $^{87}\text{Sr}/^{86}\text{Sr}(i)$ from Wilson (1989); (b) $^{87}\text{Sr}/^{86}\text{Sr}(i)$ vs. SiO_2 (wt%) and (c) $^{87}\text{Sr}/^{86}\text{Sr}(i)$ vs. $\text{P}_2\text{O}_5/\text{K}_2\text{O}$ (wt%).

Rocks of nearby ages and alkaline signatures have been reported in Brazil and Paraguay (e.g., Velázquez et al., 2006; Gomes et al., 2013). Particularly, the youngest Na-alkaline rocks from eastern Paraguay display an isotopic signature between the EMI and HIMU mantle components (Gomes et al., 2013), as the Uruguayan Ne-tephrites (Figure 7), or related to other mantle end members (Figures 8 – 9). As suggested by some authors (Comin-Chiaramonti et al., 1997; 1999; Velázquez et al., 2006), the presence of multiple sublithospheric mantle heterogeneities can be attributed to metasomatic processes that probably affected the mantle source from the Meso- to Neoproterozoic times. The origin for the mantle metasomatism that affected the southeastern South American Platform discussed by Azzone et al. (2018), could be assigned either to the infiltration of fluids related to subduction-driven processes involved in the agglutination of Gondwana in the Neoproterozoic (e.g. Heilbron and Machado, 2003; Ruberti et al., 2012), or to low melting rates of the asthenospheric mantle in an extensional environment related to the break-up of that supercontinent along the Mesozoic (Almeida, 1983; Comin-Chiaramonti and Gomes, 2005b). Evidence of metasomatism is present on the petrography of the alkaline Paraguayan rocks and their xenoliths, as well as in their geochemical and isotopic composition (Comin-Chiaramonti et al., 2009).

Also, metasomatic events have been suggested for the Paleoproterozoic to Neoproterozoic times as precursors to the alkaline and tholeiitic magmas in the Paraná-Angola-Etendeka system (Comin-Chiaramonti and Gomes, 2005b; Antonini et al., 2005; Comin-Chiaramonti et al., 2007a). Furthermore, the Uruguayan tholeiitic mafic intrusions related to the PMP, and distributed in the NB as dikes and sills reflect contributions from recycled sediments from a

stagnant slab beneath South America during Parana volcanism (Muzio et al., 2017).

However, the presence of mantle heterogeneities or end-members can be associated in space as a function of various protoliths (Comin-Chiaramonti et al., 2007b). According to Ferreira et al. (2022), the local mantle composition, depth, and crustal extension ratios determined the magma composition during the Gondwana break-up and subsequent scattering. Consequently, they concluded that this event played a prominent role in the melting processes of the metasomatized mantle during the Mesozoic-Paleogene period in South America. Considering the T_{DM} ages from 0.741 to 0.661 Ma and ϵNd_i in the range of +0.56 to +1.14 and the preliminary chemical and isotopic data presented here, we can assume that the sublithospheric mantle enrichment could correspond to both local metasomatism inherited from the Gondwana amalgamation and the Gondwana break-up event. In the latter case, magma mixing due to decompression could have occurred, involving end-member mantle components (Stracke, 2012) from an enriched mantle source.

6. CONCLUSIONS

- The evidence collected from field studies, litho geochemistry, and geochronologic data points to an unrevealed alkaline SiO_2 -undersaturated magmatic event in the northwestern region of Uruguay, particularly for the southern extreme of the PB.
- The geochemical and Sr-Nd-Pb isotopic data of the Ne-tephrites from northwestern Uruguay reinforce previous studies, ruling out a significant

participation of OIB-like mantle components in their genesis, with the possible involvement of metasomatic processes.

- These Ne-tephrites present geochemical and isotopic features similar to those of Cenozoic sodic alkaline magmatism in eastern Paraguay.
- New studies are underway to study new discoveries of these rocks, integrating the petrological and structural data to understand the geodynamic framework.

Acknowledgments

This work was supported by the *Comisión Sectorial de Investigación Científica*, UdelaR (grant CSIC-152) and *Agencia Nacional de Investigación e Innovación* (grant FCE – 156437), Montevideo. The authors are especially grateful to the anonymous reviewers and to M. Valencia-Moreno for their valuable contributions.

7. REFERENCES

- Almeida, F.F.M., 1954. Botucatu, um deserto triássico da América do Sul. DNPM Div. Geol. Min., Notas Preliminares e Estudos, 86, 21p.
- Almeida F.F.M., 1983. Relações tectônicas das rochas alcalinas mesozóicas da região meridional da plataforma sul-americana. *Revista Brasileira de Geociências*, 13, 3, 139-158.
- Antonini, P., Gomes, C. B., Gasparon, M., Comin-Chiaramonti, P. 2005. Post-paleozoic magmatism in eastern Paraguay: Sr-Nd-Pb isotope compositions. In *Mesozoic to Cenozoic alkaline magmatism in the Brazilian platform*. São Paulo, EDUSP/FAPESP, 57-69.

Azzone, R. G., Ruberti, E., Lopes da Silva, J.L., Gomes, C.B., Rojas, G.E.E., Hollanda, M.H.B., Tassinari, C.C.G., 2018. Upper Cretaceous weakly to strongly silica-undersaturated alkaline dike series of the Mantiqueira Range, Serra do Mar alkaline province: Crustal assimilation processes and mantle source signatures. *Brazilian Journal of Geology*, 48, 2, 373-390. DOI: 10.1590/2317-4889201820170089.

Bailey, D.K. 1987. Mantle metasomatism--perspective and prospect. In: Fitton, J.G. and Upton, B.G.J. (eds.), *Alkaline Igneous Rocks*. Geological Society, London, Special Publications, 30, 1-13.
<https://doi.org/10.1144/GSL.SP.1987.030.01.02>

Barbieri, M., Beccaluva, L., Brotzu, P., Conte, A., Garbarino, C., Gomes, C. B., Loss, E., Macciotta, Morbidelli, L., Scheibe, L. F., Tamura, R. M. and Traversa, G., 1987. Petrological and geochemical studies of alkaline rocks from continental Brazil. 1. The phonolite suite from Piratini, RS. *Geochimica Brasiliensis*, v1, 109-138.

Beccaluva, L., Bianchini, G., Ellam, R. M., Marzola, M., Oun, K. M., Siena, F., Stuart, F.M., 2008. The role of HIMU metasomatic components in the North African lithospheric mantle: petrological evidence from the Gharyan lherzolite xenoliths, NW Libya. *Geological Society, London, Special Publications*, 293, 253-277. <https://doi.org/10.1144/SP293.12>

Biondi, J.C., 2005. Brazilian mineral deposits associated with alkaline and alkaline-carbonatite complexes. In: Comin- Chiaramonti, P., Gomes, C. B. (Eds.) *Mesozoic to Cenozoic Alkaline Magmatism in The Brazilian Platform*, São Paulo, EDUSP/FAPESP, 707 – 750.

Bossi, J., 1966. Geología del Uruguay. Departamento de Publicaciones, Universidad de la República, Montevideo, 469 p.

Boynnton, W., 1984. Geochemistry of the rare earth elements: meteorite studies. In: Henderson, H. (Ed.), Rare Earth Element Geochemistry, Elsevier, Amsterdam, 63-114.

Bryan, S.E., Ernst, R.E., 2008. Revised definition of Large Igneous Provinces (LIPs). Earth Science Reviews, 86, 1-4, 175-202. DOI: 10.1016/j.earscirev.2007.08.008.

Burger Jr. C.; Ribeiro, M. and Gerhardt, A.L.B., 1988. On the alkaline rocks of Piratini, Rio Grande do Sul, Brazil. Paula-Coutiana, Porto Alegre. v2, 81-112.

Carlson R.W., Hart W.K., 1987. Crustal genesis on the Oregon Plateau. Journal of Geophysical Research, 92, 6191-6206.

Cernuschi, F., Dilles, J.H., Kent, A.J., Schroer, G., Raab, A.K., Conti, B., Muzio, R., 2015. Geology, Geochemistry and Geochronology of the Cretaceous Lascano East Intrusive Complex and Magmatic Evolution of the Laguna Merín Basin, Uruguay. Gondwana Research, 28, 837-857.

Coffin, M., Eldholm, O., 1994. Large igneous provinces: crustal structure, dimensions, and external consequences, Reviews of Geophysics, 32, 1, 1-36. DOI:10.1029/93RG02508.

Comin-Chiaramonti P., Castorina F., Cundari A., Petrini R., Gomes, C.B. 1995. Dykes and sills from Eastern Paraguay: Sr and Nd isotope systematics. In: Baer G., Heimann A. (eds.), Physics and chemistry of dykes. Rotterdam, Balkema, p. 267-278.

Comin-Chiaramonti, P., Civetta, L., Petrini, P., Piccirillo, E.M., Bellieni, G., Censi, P., Bitschene, P.R., Demarchi, D., De Min, A., Gomes, C.B., Castillo, A.M.C.,

Velázquez, J.C., 1991. Tertiary nephelinitic magmatism in eastern Paraguay: petrology, Sr-Nd isotopes and genetic relationships with associated spinel peridotite xenoliths. *European Journal of Mineralogy*, 3, 507-525.

Comin-Chiaramonti, P., Cundari, A., De Graff, J.M., Gomes, C.B., Piccirillo, E.M., 1999. Early Cretaceous-Tertiary magmatism in Eastern Paraguay (western Parana basin): geological, geophysical and geochemical relationships. *Journal of Geodynamics*, 28, 375-391.

Comin-Chiaramonti, P., Cundari, A., Piccirillo, E.M., Gomes, C.B., Castorina, F., Censi, P., De Min, A., Marzoli, A., Speziale, S. and Velázquez, V.F., 1997. Potassic and sodic igneous rocks from Eastern Paraguay: their origin from the lithospheric mantle and genetic relationships with the associated Paraná flood tholeiites. *Journal of Petrology*, 38, 495-528.
<https://doi.org/10.1093/petroj/38.4.495>

Comin-Chiaramonti, P., De Min, A., Cundari, A., Girardi, V., Ernesto, M., Gomes, C., Riccomini, C., 2013. Magmatism in the Asunción-Sapucaí-Villarrica Graben (Eastern Paraguay) revisited: Petrological, Geophysical, Geochemical, and Geodynamic Inferences. *Journal of Geological Research*, Article ID 590835, 22p.
<http://dx.doi.org/10.1155/2013/590835>.

Comin-Chiaramonti, P., Gomes, C. B., 2005a. An introduction to the alkaline and alkaline-carbonatitic magmatism in and around the Paraná basin. In: Comin-Chiaramonti, P., Gomes, C. B. (Eds.) *Mesozoic to Cenozoic Alkaline Magmatism in The Brazilian Platform*, São Paulo, EDUSP/FAPESP, 21-30.

Comin-Chiaramonti, P., Gomes, C.B., 2005b. *Mesozoic to Cenozoic Alkaline Magmatism in the Brazilian Platform*. EDUSP/FAPESP (Ed.), São Paulo, Brazil, 737 p.

Comin-Chiaramonti, P., Gomes, C.B., De Min, A., Ernesto, M., Marzoli, A. and Riccomini, C., 2007a. Eastern Paraguay: an overview of the post-Paleozoic magmatism and geodynamic implications. *Rendiconti Fis. Acc. Lincei, serie IX*, vol. XVIII, 139-192.

Comin-Chiaramonti, P., Lucassen, F., Girardi, V.A.V., De Min, A., Gomes, C.B., 2009. Lavas and their mantle xenoliths from intracratonic eastern Paraguay (South America Platform) and Andean Domain, NW-Argentina: a comparative review. *Mineralogy and Petrology*, 98, 143-165. DOI 10.1007/s00710-009-0061-6.

Comin-Chiaramonti, P., Marzoli, A., Gomes, C.B., Milan, A., Riccomini, C., Velázquez, V.F., Mantovani, M.M.S., Renne, P., Tassinari, C.C.G., Vasconcelos, P.M., 2007b. The origin of Post-Paleozoic magmatism in Eastern Paraguay. In: Foulger, R.G., Jurdy, D.M. (Eds.) *Plates, plumes and planetary processes*. Geological Society of America, 430 (Special Paper), pp. 603-633. Doi: 10.1130/2007.2430(29).

Cordani, U.G.; Neves, B.B.B.; Fuck, R.A.; Porto, R.; Thomaz Filho, A.; Cunha, F.M.B., 1984. Estudo preliminar de integração do Pré-Cambriano com os eventos tectônicos das bacias sedimentares brasileiras. Rio de Janeiro: PETROBRÁS, Série Ciência-Técnica-Petróleo, 15, 70 p.

Creer, K.M., Miller J.A., Gilbert-Smith A., 1965. Radiometric age of the Serra Geral Formation. *Nature*, 207, 282 – 283. DOI:10.1038/207282a0.

Da Silva, M.D., 2018. Novos estudos petrográficos e geoquímicos sobre a suíte alcalina Passo da Capela, Piratini – RS. Graduation thesis, Instituto de Geociências, UFRGS, Brazil, 112 p.

De Graff, J.M., 1985. Late Mesozoic crustal extension and rifting on the western edge of the Paraná Basin, Paraguay. Geological Society of America, Abstracts with Programs, 17, p. 560.

De Paolo, D.J., 1981. Nd isotopic studies: Some new perspectives on Earth Structure and Evolution. Earth and Space Science News, 62,137-145.

De Paolo, D.J., Wasserburg, G.J., 1979. Sm-Nd age of the Stillwater complex and the mantle evolution curve for neodymium. Geochimica et Cosmochimica Acta, 43, 7, 999 – 1008. [https://doi.org/10.1016/0016-7037\(79\)90089-9](https://doi.org/10.1016/0016-7037(79)90089-9)

Féraud, G., H., Martínez, M., Ures, C., Schipilov, A., Bossi, J., 1999. $^{40}\text{Ar}/^{39}\text{Ar}$ age and geochemistry of the southern extension of Paraná traps in Uruguay. In: II Simposio Sudamericano de Geología Isotópica, Córdoba, Argentina, 57-59.

Ferreira, A.C.D., Conceicao, R.V. and Misuzaki, A.M.P., 2022. Mesozoic to Cenozoic alkaline and tholeiitic magmatism related to West Gondwana break-up and dispersal. Gondwana Research, 106, 15 – 33. <https://doi.org/10.1016/j.gr.2022.01.005>

Fletcher, C.J.N., Beddoc-Stephens, B.,1987. The petrology and crystallization history of the Velasco alkaline province, eastern Bolivia. En: Fitton, J.G. y Upton, B.G.J. (Eds.) Alkaline igneous rocks. Geological Society of London, Special Publication 30, pp. 403-413

Gomes, C.B., Comin-Chiaramonti P., 2017. Magmatismo alcalino continental da região meridional da Plataforma Brasileira. São Paulo, Edusp/Fapesp, 608 p.

Gomes, C.B., Comin-Chiaramonti, P., Velázquez, V.F., 2013. A synthesis on the alkaline magmatism of Eastern Paraguay. Brazilian Journal of Geology, 43, v.4, 745-761. DOI: 10.5327/Z2317-488920130004000012.

Gomes, C.B., Laurenzi, M.A., Censi, P.; De Min, A., Velázquez, V.F., Comin-Chiaramonti, P., 1996. Alkaline magmatism from northern Paraguay (Alto Paraguay): a Permo-Triassic Province. In: Comin-Chiaramonti, P.; Gomes, C.B. (Eds.): Alkaline magmatism in central-eastern Paraguay. Relationships with coeval magmatism in Brazil, Edusp-Fapesp, São Paulo, Brazil, 223-230.

Gomes, C.B., Milan, A., Velázquez, V.F., Riccomini, C., Comin-Chiaramonti, P., Vasconcelos, P.M., Tassinari, C.C.G., 2003. Magmatismo alcalino da porção centro-oriental do Paraguai: novos dados geocronológicos para as rochas das províncias Central e Assunção. 7º Congresso de Geoquímica dos Países de Língua portuguesa, Resumos, Maputo, p. 34.

Hamilton, P. J., O'nions, R. K., Bridgewater, D., Annutman, A., 1983. Sm-Nd studies of Archaean metasediments and metavolcanics from West Greenland and their implications for the Earth's early history. *Earth and Planetary Science Letters*, 62, 263–272.

Hart, S.R., 1984. A large-scale isotope anomaly in the Southern Hemisphere mantle, *Nature*, 309, 753 – 757.

Hart. W.K., Carlson R.W., Shirley S.B., 1997. Radiogenic Os in primitive basalts from the northwestern U.S.A.: implications for petrogenesis. *Earth and Planetary Science Letters*, 150, 103-116.

Heilbron, M., Machado, N., 2003. Timing of terrane accretion in the Neoproterozoic–Eopaleozoic Ribeira orogen (SE Brazil). *Precambrian Research*, 125, 1-2, 87-112.

Huang, H.M., Hawkesworth, C.J., Van Calsteren, P., McDermott, F., 1995. Geochemical characteristics and origin of the Jacupiranga carbonatites, Brazil. *Chemical Geology*, 119, 79-99.

Janasi, V.A., de Freitas, V.A., Heaman, L.H., 2011. The onset of flood basalt volcanism, Northern Paraná Basin, Brazil: A precise U–Pb baddeleyite/zircon age for a Chapecó-type dacite. *Earth and Planetary Science Letters*, 302, 147 – 153. DOI: 10.1016/j.epsl.2010.12.005.

Janousek, V., Farrow, C.M., Erban, V., 2006. Interpretation of whole-rock geochemical data in igneous geochemistry: introducing Geochemical Data Toolkit (GCDkit). *Journal of Petrology*, 47, 6, 1255-1259.

Lagorio, S.L., Vizán, H., Geuna, S.E., 2016. Early Cretaceous Volcanism in Central Argentina. In: Lagorio S.L., Vzán H., Geuna S.E.(Eds.). *Early Cretaceous Volcanism in Central and Eastern Argentina During Gondwana Break-Up*. Springer Briefs in Earth System Sciences. Springer. Chap. 2, 9-86.

Le Bas, M., Le Maitre, R., Streckeinsen, A., Zanettin, B., 1986. A chemical classification of volcanic rocks based on the total alkali-silica diagram. *Journal of Petrology*, 27, 745-750.

Le Maître, R.W., 2002. A classification of igneous rocks and glossary of terms. Recommendations of the IUGS subcommission on the systematic of de Igneous Rocks. Cambridge University Press, 2 Ed., 252 p.

Litherland, M., Annells, R.N., Appleton, J.D., Berrange, J.P., Bloomfield, K., Burton, C.C.J., Darbyshire, D.P.F., Fletcher, C.J.N., Hawkins, M.P., Klinck, B.A., Llanos, A., Mitchell, W.I., O'Connor, E.A., Pitfield, P.E.J., Power, G., Webb, B.C., 1986. The geology and mineral resources of the Bolivian Precambrian shield. *British Geological Survey Overseas Memoir*. 9, 153p.

Lustrino, M., Melluso, L., Brotzu, P., Gomes, C.B., Morbidelli, L., Muzio, R., Ruberti, E., Tassinari, C.C.G., 2005. Petrogenesis of the Early Cretaceous Valle Chico igneous complex SE Uruguay: relationships with Parana-Etendeka Province. *Lithos* 82, 407–434. <https://doi.org/10.1016/j.lithos.2004.07.004>.

Menzies, M., Murthy, V.R., 1980. Mantle metasomatism as a precursor to the genesis of alkaline magmas-isotopic evidence, *American Journal of Science*, Vol. 280-A, 622-638.

Middlemost, E., 1975. The Basalt Clan. *Earth-Science Reviews*, 11, 337-564. [http://dx.doi.org/10.1016/0012-8252\(75\)90039-2](http://dx.doi.org/10.1016/0012-8252(75)90039-2)

Milani, E.J., Melo, J.H.G., Souza, P.A., Fernandes, L.A., França, A.B., 2007. Bacia do Paraná. *Boletim de Geociências da Petrobras*, 15, 2, 265-287.

Milner, S.C., Le Roex, A.P., O'Connor, J.M., 1995. Age of Mesozoic igneous rocks in northwestern Namibia, and their relationship to continental break-up, *J. Geol. Society London*, 152, 97-104.

Muzio, R., 2000. Evolução petrológica e geocronologia do maciço alcalino Valle Chico, Uruguai. Ph.D. thesis, Universidade Estadual Paulista, Brazil, 171 p.

Muzio, R., Olivera, L., Peel, E., Fort, S., 2019. Geochemical features of alkaline volcanism in the southern extreme of Paraná Basin, NW Uruguay. *Goldschmidt Conference Abstracts*, Barcelona, Spain, <https://goldschmidt.info/abstracts/abstractSearch>.

Muzio R., Peel, E., Porta, N., Scaglia, F., 2017. Mesozoic dykes and sills from Uruguay: Sr - Nd isotopes and trace element geochemistry. *Journal of South American Earth Sciences*, 77, 92–107. <http://dx.doi.org/10.1016/j.jsames.2017.04.016>.

Olivera, L., 2019. Petrología de rocas volcánicas al Norte de Pepe Núñez (Depto. de Salto). Graduation thesis, Instituto de Ciencias Geológicas, Facultad de Ciencias, UdelaR, Montevideo, 97 p.

Olivera, L., Muzio, R., 2019. Petrografía del magmatismo alcalino en la Cuenca Norte uruguaya (departamento de Salto). Revista de la Sociedad Uruguaya de Geología, 22, 27-48, <https://www.sociedadgeologiauy.org/revista-no-22-2019>.

Pearce, J.A., 2008. Geochemical fingerprinting of oceanic basalts with applications to ophiolite classification and the search for Archean oceanic crust. Lithos, 100, 14-48.

Peate, D.W., 1997. The Parana magmatic province. In: Mahoney, J.J., Coffin, M.F. (Eds.), Large Igneous Provinces: Continental, Oceanic and Planetary Flood Volcanism, Geophysical Monograph, 100, 217-245.

Philipp, R.P., Viero, A.P., Comin-Chiaramonti, P., Gomes, C.B., 2005. Mesozoic alkaline rocks of Rio Grande do Sul. In: Comin-Chiaramonti, P. and Gomes, C.B. (Eds.). Mesozoic to Cenozoic alkaline magmatism in the Brazilian platform. São Paulo, Edusp/Fapergs, 573-590.

Piccirillo, E.M., Melfi, A.J., 1988. Appendix – Rare Earth Elements, L.S. Marques analyst. In: MacDougall, J.D. (ed.). Continental Flood Volcanism from the Paraná Basin, Universidade de São Paulo, 501-504.

Piccirillo, E.M., Melfi, A.J., Comin-Chiaramonti, P., Bellieni, G., Ernesto, M., Marques, L.S., Nardy, A.J.R., Pacca, I.G., Roisenberg, A., Stolfa, D., 1988. Continental Flood Volcanism from the Paraná Basin (Brazil). In: MacDougall, J.D. (ed.). Continental Flood Basalts: Petrology and Structural Geology, San Diego, California, USA, 195-238.

Preciozzi, F., Spoturno, J., Heinzen, W., Rossi, P., 1985. Memoria Explicativa de la Carta Geológica del Uruguay a escala 1/500 000. DINAMIGE-M.I.E.M. Montevideo, 72 p.

Renne, P.R., Ernesto, M., Pacca, I.G., Coe, R.S., Glen, J.M., Prévot, M., Perrin, M., 1992. The age of Parana flood volcanism, rifting of Gondwanaland, and the Jurassic-Cretaceous boundary. *Science*, 258, 975-979.

Renne, P.R., Mertz, D.F., Ernesto, M., Marques, L.S., Teixeira, W., Ens, H.H., Richards, M.A., 1993. Geochronologic constraints on magmatic and tectonic evolution of the Paraná Province. American Geophysical Union abstract, EOS, 74, 553.

Renner, L.C., Hartmann, L.A., Wildner, W., Massone, H.J., Theye, T., 2011. A microanalytical approach to partition coefficients in plagioclase and clinopyroxene of basaltic sills in Serra Geral Formation, Paraná Basin, Brazil. *Revista Brasileira de Geociências*, 41, 2, 263 – 289.

Ribeiro, M., 1971. Uma província alcalina no Rio Grande do Sul – I Estudos Preliminares. *Lheringia*, v4, 59-71.

Riccomini, C., Velázquez, V.F., Gomes, C.B., 2001. Cenozoic lithospheric faulting in the Asunción rift, Eastern Paraguay. *Journal of South American Earth Sciences*, 14, 625 – 630.

Riccomini, C., Velázquez, V.F., Gomes, C.B., 2005. Tectonic controls of the Mesozoic and Cenozoic alkaline magmatism in central-southeastern Brazilian platform. In: Comin-Chiaramonti, P., Gomes, C.B. (eds.), *Mesozoic to Cenozoic alkaline magmatism in the Brazilian Platform*, Edusp/Fapesp, São Paulo, 31-56.

Roden M.F., Murthy V.R., 1985. Mantle metasomatism. *Annual Review of Earth and Planetary Sciences*, 18, 269 – 296.

Rossello, E.A., De Santa Ana, H.; Veroslavsky, G., 2000. El Lineamiento Santa Lucía-Aiguá-Merín (Uruguay): Un corredor tectónico extensivo y transcurrente dextral precursor de la apertura Atlántica. *Revista Brasileira de Geociências*, 30, 749 - 756.

Ruberti E., Rojas G.E.E., Azzone R.G., Comin-Chiaramonti P., de Min A., Gomes C. 2012. The Banhadão alkaline complex, southeastern Brazil: Source and evolution of potassic SiO₂-undersaturated high-Ca and low-Ca magmatic series. *Mineralogy and Petrology*, 104, 63-80.

Rudnick, R.L., Fountain, D.M., 1995. Nature and Composition of the Continental-Crust—a Lower Crustal Perspective. *Reviews of Geophysics*, 33, 3, 267-309. DOI: 10.1029/95RG01302.

Salamuni, R., Bigarella, J., 1967. The Botucatú Formation. In: Bigarella, J., R. Becker & I. Pinto (Eds.): *Problems in Brazilian Gondwana Geology*, Curitiba, Brazil, 197-206.

Soto, M., 2014. Geología, geofísica y geoquímica de la región de Pepe Núñez, Cuenca Norte (Uruguay). M.Sc. thesis, Instituto de Ciencias Geológicas, Facultad de Ciencias, UdelaR, Montevideo, 248 p.

Stracke, A., 2012. Earth's heterogeneous mantle: A product of convection-driven interaction between crust and mantle. *Chemical Geology*, 330-331, 274 – 299. <http://dx.doi.org/10.1016/j.chemgeo.2012.08.007>

Sun, S., McDonough, W., 1989. Chemical and isotopic systematics of ocean basalts: implications for mantle composition and processes. In: Saunders, A.,

Norry, M. (Eds.), Magmatism in Ocean Basins, Geological Society of London, Special Publication, 42, 313-345. doi: 10.1144/GSL.SP.1989.042.01.19.

Turner, S. P., Peate, D. W., Hawkesworth, C. J., Mantovani, M. S. M. 1999. Chemical stratigraphy of the Parana basalt succession in western Uruguay: further evidence for the diachronous nature of the Parana magma types. *Journal of Geodynamics*, 28, 4-5, 459-469. [https://doi.org/10.1016/S0264-3707\(99\)00021-6](https://doi.org/10.1016/S0264-3707(99)00021-6)

Ucha, N., de Santa Ana, H., 1994. Exploration perspectives and hydrocarbon potential of the Uruguayan sedimentary basins. ANCAP Report, Montevideo, 90 p.

Ulbrich, H.H.G.J., Gomes, C.B., 1981. Alkaline rocks from continental Brazil. *Earth Science Reviews*, 17, 135-154.

Velázquez, V.F., Comin-Chiaramonti, P., Cundari, A., Gomes, C.B., Riccomini, C., 2006. Cretaceous Na-Alkaline Magmatism from the Misiones Province (Paraguay): Its relationships with the Paleocene Na-alkaline analog from Asunción and geodynamic significance. *Journal of Geology*, 114, 5, 593-614.

Vieira Jr., N., 1985. Petrologia e geoquímica do vulcanismo mesozóico do Jaguarão, RS. M.S. tesis, UFRGS, Brazil, 136 p.

Viero, A.P., 1998. O Magmatismo máfico alcalino Mesozóico do Rio Grande do Sul. PhD. thesis, UFRGS, Brazil, 249 p.

Wilson, M., 1989. Igneous petrogenesis, a global tectonic approach. Springer, 466 p. <https://doi.org/10.1007/978-94-010-9388-0>

Zindler, A., Hart, S., 1986. Chemical geodynamics. *Annual Rev. Earth and Planetary Sciences*, 14, 493-571.

FIGURE CAPTIONS

Figure 1 – Simplified geological map of the Paraná Basin, with the regional location of the Paraná Magmatic Province (modified after Piccirillo et al., 1988; Renner et al., 2011).

Figure 2 – (a) Location map with the main structural framework and (b) simplified geological map of the study region, northwestern Uruguay (Olivera, 2019).

Figure 3 – Classification diagram for the Ne-tephrites, according to Le Bas et al. (1986).

Figure 4 – Classification diagram for the Ne-tephrites, according to the distribution of K_2O vs. Na_2O (Middlemost, 1975). The shaded areas represent average values for the Na-alkaline rocks of Asunción (Eocene) and Piratini Provinces (Late Cretaceous); taken from Comin-Chiaramonti et al. (1991); Comin-Chiaramonti et al. (2013) and da Silva (2018).

Figure 5 – Multielement diagram and REE patterns for the Ne-tephrites normalized according to (a) Primitive mantle (Sun and Mc Donough, 1989); (b) Chondrite (Boynnton, 1984). The shaded areas in green represent average values for the Na-alkaline rocks of Asunción, taken from Comin-Chiaramonti et al. (1991); Comin-Chiaramonti et al. (2013).

Figure 6 - (a) Th/Yb vs. Nb/Yb and (b) TiO_2 vs. Nb/Yb incompatible element ratio diagrams for the Ne-tephrites, after Pearce (2008).

Figure 7 – Initial $^{87}Sr/^{86}Sr$ vs. $^{143}Nd/^{144}Nd$ diagram for the Ne-tephrites from Uruguay, modified after De Paolo and Wasserburg (1979) and Zindler and Hart (1986). The shaded area in green represents average values for contemporary sodic alkaline rocks from Paraguay (taken from Gomes et al., 2013). References: MORB: Mid Ocean Ridge Basalts, DM: Depleted Mantle, MA-OIB: Mantle Array-

Ocean Island Basalts, BSE: Bulk Silicate Earth, HIMU: High μ mantle component ($\mu=^{238}\text{U}/^{204}\text{U}$), EM (I, II): Enriched Mantle.

Figure 8 – (a) $^{207}\text{Pb}/^{204}\text{Pb}$ vs. $^{206}\text{Pb}/^{204}\text{Pb}$ and (b) $^{208}\text{Pb}/^{204}\text{Pb}$ vs. $^{206}\text{Pb}/^{204}\text{Pb}$ isotope compositions for the Ne-tephrites compared to mantle components (Zindler and Hart, 1986). NHRL – Northern Hemisphere Reference Line (Hart, 1984). The shaded area in green represents average values for contemporary sodic alkaline rocks from Paraguay (taken from Gomes et al., 2013). References: MORB: Mid Ocean Ridge Basalts, DM: Depleted Mantle, BSE: Bulk Silicate Earth, PREMA: Prevalent Mantle, EM (I, II): Enriched Mantle.

Figure 9 – (a) $^{87}\text{Sr}/^{86}\text{Sr}_{(i)}$ vs. $^{206}\text{Pb}/^{204}\text{Pb}$ and (b) $^{143}\text{Nd}/^{144}\text{Nd}_{(i)}$ vs. $^{206}\text{Pb}/^{204}\text{Pb}$ isotope compositions for the Ne-tephrites compared to the fields of mantle components (Zindler and Hart, 1986). The shaded area in green represents average values for contemporary sodic alkaline rocks from Paraguay (taken from Gomes et al., 2013). References: MORB: Mid Ocean Ridge Basalts, DM: Depleted Mantle, BSE: Bulk Silicate Earth, PREMA: Prevalent Mantle, EM (I, II): Enriched Mantle, HIMU: High μ mantle component ($\mu=^{238}\text{U}/^{204}\text{U}$).

Figure 10 – Indicative diagrams to evaluate crustal contamination. (a) Ba/Yb vs. $^{87}\text{Sr}/^{86}\text{Sr}_{(i)}$ from Wilson (1989); (b) $^{87}\text{Sr}/^{86}\text{Sr}_{(i)}$ vs. SiO_2 (wt%) and (c) $^{87}\text{Sr}/^{86}\text{Sr}_{(i)}$ vs. $\text{P}_2\text{O}_5/\text{K}_2\text{O}$ (wt%).

Table Captions

Table 1 – Results of K-Ar dating (whole rock).

Table 2 – Geochemical data for the Ne-tephrites from northwestern Uruguay.

Table 3 – Sr - Nd – Pb isotopic compositions for the Ne-tephrites from northwestern Uruguay. Initial ratios for Sr, Nd and epsilon values were calculated to a mean age of 57.6 Ma.